

CENTRALLY PRESTRESSED CONCRETE COLUMNS AND PILES WITHOUT MILD-STEEL REINFORCEMENT

D.V. Reddy, PhD, P.E., Civil Engineering, Florida Atlantic University, Boca Raton, FL
Rathinam Periyaiyah, Sea Engineering Inc., Houston, TX

ABSTRACT

The Centrally Prestressed Concrete Columns and Piles without Mild-Steel Reinforcement (CPCWMR) column and pile design is an innovative idea, by which the innate incompatibility between concrete and steel is eliminated by removal of the latter; but flexural resistance and ductility are restored by the application of a centrally located prestressing tendon or closely spaced strands. This concentration of steel results in a significant increase in concrete cover for better corrosion protection without loss in strength. The practical applicability of the CPCWMR column design concept is substantiated by an inelastic analysis. A series of columns are tested and the test results showed higher ultimate strength and ductility compared to the conventional columns.

A modified Freyssinet type hinge, called Extended Flexural Device for CPCWMR column, is conceived to meet the increased ductility demand of CPCWMR column in the seismic region. Hinge test shows an excellent energy dissipating characteristics.

Keywords: Centrally Prestressed Concrete Columns and Piles without Mild-Steel Reinforcement, CPCWMR, pile, inelastic analysis, hinge.

RESEARCH SIGNIFICANCE

It has been observed that the compressive resistance of axially loaded reinforced concrete components is invariably less than the sum of individual strengths of the constituent concrete and steel elements due to structural incompatibility in the inelastic phase. Structural instability, at or near ultimate limit states in traditionally reinforced concrete columns, renders accurate prediction of their resistance, difficult. This unreliability, exacerbated by the fact that loading of columns without eccentricity is practically impossible, causes design codes to specify severe resistance factors in order to assure a desirable safety level. Structural reliability is further impaired by the probability of spalling of the concrete cover due to corrosion of the reinforcement.

INTRODUCTION

Reinforced concrete structures have been widely used in past years due to their composition of slender, lighter, and longer span members with increased flexural capacity, energy absorption capacity, and resilience.

Increased concerns about the application of reinforced concrete members as compression members, especially in corrosive and seismic environments, has been expressed by many researchers and practicing engineers. The basic concerns are its inherent material nonhomogeneity, corrodable rebar's traditional perimetrical location, and column beam connections. The increase in airborne corrosive chemicals and percolation of salt laden water causes corrosion of the reinforcement. The cracks formed along the rebars due to corrosion tend to reduce the effective area of the column and the degree of restraint that the covering concrete provides to the steel bars, thus reducing column strength. This reduction has been reported up to 30%, Uomoto and Misra (1988).

Many investigators are undergoing studies of the corrosion problem and viable remedies for reinforced concrete bridge columns. Investigators, Uomoto and Misra (1988), and Ranade and Reddy (1994), recommended that the increase of the concrete cover is effective in solving the corrosion problem in reinforced concrete columns. However, the increased concrete cover leads to the potential structural instability of reinforced concrete column due to reduction in effective confined area. The tendency of ties bending outward, the arching action between steel bars, and the reduction in the effectively confined sectional area, Figure 1, leading to reduction in strength and ductility, was identified by Sheikh and Uzumeri (1980), Mander, Priestley, and Park (1988), and Cusson and Paultre (1994). Razvi and Saatcioglu (1994) indicated that effective confinement can be improved by closer ties, but this increases the susceptibility of cover separation. Ichinose (1996) pointed out that reversed cyclic loading often causes splitting bond failure in reinforced concrete columns.

On the other hand, Zia and Moreadith (1966) concluded that prestressed columns and piles, especially those subjected to large load eccentricity, offer high strength and ductility.

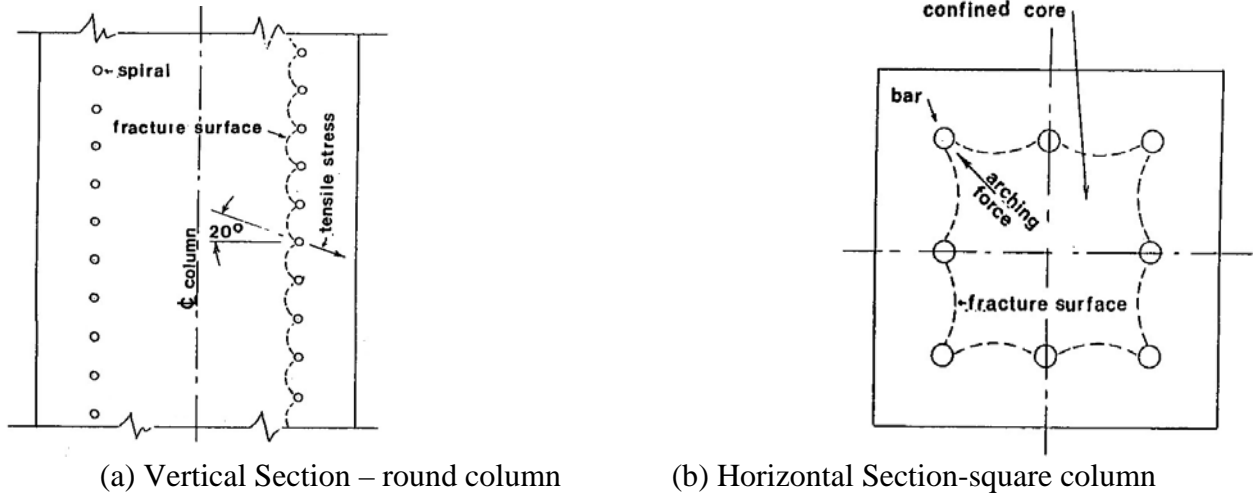


Figure 1 Observed spalling of concrete covers

Elias and Durrani (1988) and Carinci and Halvorsen (1987) reported that lateral reinforcement does not have any effect on the load carrying capacity of prestressed columns, and recommended elimination of the 0.85 strength reduction factor, since the concrete in such columns without ties is able to reach its theoretical ultimate strength value. One cumulative argument that can be derived from these studies is that the good performance of prestressed concrete columns is not conditional upon the presence of ties.

In fact, as the prestressing strands are in a state of high axial tension (approximately 6,000 microstrain), there is no possibility of premature strand buckling as the concrete approaches failure (approximately 3,600 microstrain). But, the elimination of ties or spirals does not resolve the corrosion problem of the strands. The first innovative idea of this project is the relocation of all prestressing strands into a central location by which the concrete cover is increased to the possible maximum. Typical cross sections of the centrally prestressed unreinforced concrete (CPCWMR) piles and columns are displayed in Figure 2. For the same level of prestress, the strands of the traditional pile design are simply moved into a central 2.0 in. (50.8mm) grid pattern, similar to beams, and without ties. In the CPCWMR column, the strands are banded into a post-tensioning tendon, located in a central duct. The tendon can be loop-anchored in the substructure and the post-tensioning is carried out from the top of the superstructure, thus connecting the three components together.

The first reaction of nearly all engineers to the CPCWMR concept is the fear of losing flexural resistance. As illustrated in Figure 3, this is not the case. In the traditional layout, strands only in lines “b” and “c” can reach yield point, while the stresses in strands along line “a” are barely above the prestress due to their closeness to the neutral axis. In the CPCWMR layout, all of the eight strands attain the yield level, and although the internal moment arm for the yielded strands decreases, the ultimate CPCWMR flexural resistance of 2,795 k.in. (315.78 kN-m) exceeds that of the traditional pile with 2,720 k.in. (307.3 kN-m). The above values are based on the rectangular Whitney stress block as being slim first approximations.

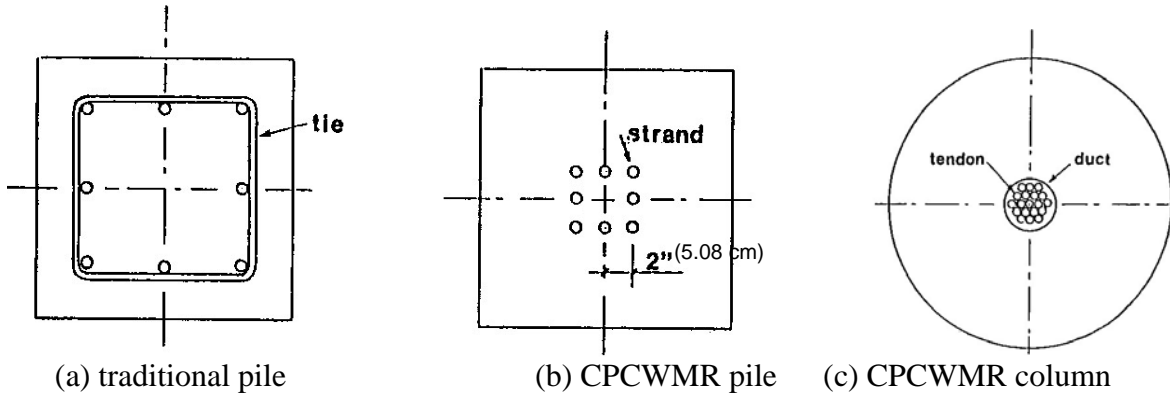


Figure 2 Traditional and proposed cross sections

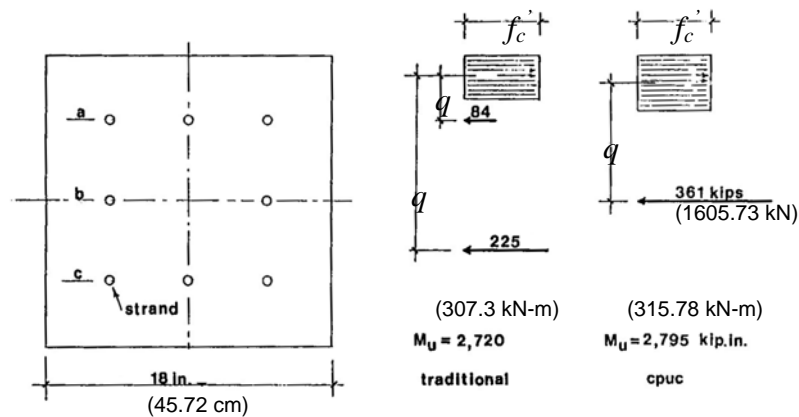


Figure 3 Comparison of flexural resistance

In areas of high seismic activity, the ductility and energy absorbing capacity that can be derived from reinforced concrete columns are often not adequate to satisfy the requirements. The second innovative concept is the combining of the CPCWMR column, having all its steel centrally located, with an inelastic device with extended flexural capability. This extended performance flexural device is not an isolator, but a completely structural device intended for connecting pier columns to either the superstructure or the substructure, or both, (see Figure 4) and transmitting considerable moments while permitting large rotations. Test results on individual hinges presented in this paper show that this inelastic device offers structural compatibility with the CPCWMR column, reduction in seismic force effect by two-thirds, tolerance of repetitive action without damage, and resistance to transient loads without excessive deformation.

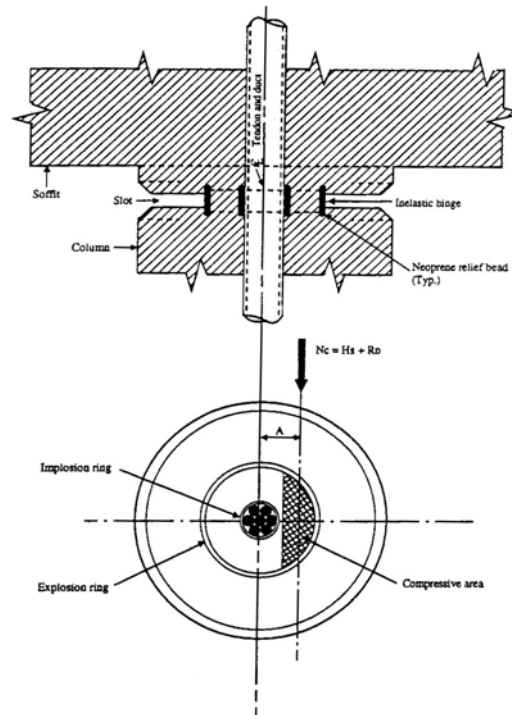


Figure 4 Modified Freyssinet type hinge

Inelastic Analysis of CPCWMR Columns

In reality, the purely axial loading on columns and piles is physically impossible; therefore, they must be analyzed for combinations of axial load and moment. The inelastic analysis of the performance of eccentrically loaded columns is rather difficult for a variety of reasons. For every increment in the concrete strain, a change will take place in the following:

- a. distribution of compressive stresses,
- b. position of the neutral axis,
- c. shape of the compressive area of the cross section for circular columns and for biaxial flexure of rectangular columns, and
- d. elastic-inelastic strain distribution in the steel.

The LRFD Code specifies that the resistance of concrete components shall be based on the conditions of force equilibrium and strain compatibility, with the strain being directly proportional to the distance from the neutral axis. The concrete compressive stress-strain distribution may be assumed to be rectangular, parabolic, or any other shape, which results in a prediction of strength in substantial agreement with test results. One such “other” shape is represented by an exponential function. Unfortunately, the associated numerical process was so cumbersome and inaccurate that it was not accepted for engineering applications in spite of the fact that it seems to offer the best correlation with test results.

The exponential relationship has recently been reviewed and found to be eminently suitable for the inelastic analysis of eccentrically loaded columns and piles. The basic independent variable of this numerical system is the ratio “ α ” between the actual concrete strain ϵ and the strain ϵ_c associated with f'_c . As illustrated in Figure 5, “ α ” uniquely defines the distribution of compressive stresses. It can be seen that at $\alpha=0.2$, the distribution is virtually linear, at $\alpha=0.6$, inelastic behavior begins to show, and at $\alpha=1.0$, inelastic distribution prevails. The curve at $\alpha=1.4$ is what can be obtained by careful and precise compressive testing of short prismatic concrete specimens; it normally signifies the extent of their strain capacity. For medium strength concretes, the Hognestad limit approximates $\alpha=1.25$. Figure 5 also explains how the curves develop.

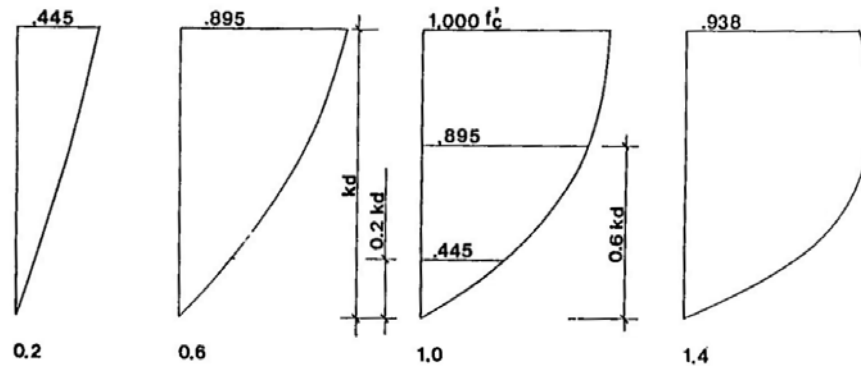


Figure 5 Distribution of compressive stresses as function of α (= 0.2, 0.6, 1.0, and 1.4)

For introduction, an 18in x 18 in CPCWMR pile will be analyzed. For rectangular cross sections in uniaxial flexure, the exponential function provides close form solutions for the compressive force N_c and its first moment M_c relative to the neutral axis. The CPCWMR column simplifies the calculations as the steel can be assumed to be bundled at its center.

Figure 6 illustrates the unfactored axial load - moment interaction curve for an 18.0 in. (45.72 cm) square pile of 6,000 psi (41370 kN/m²) concrete with eight 0.5 in. (1.27 cm) diameter, 270 ksi (1861650 kN/m²) strands. The curve is discontinued at an eccentricity of 2.0 in. (50.8 mm), as the authors tend to believe that the minimum design offset should be the larger of 2.0 in. (50.8 mm) and one tenth of the outside dimension of the pile (1.8 in. (45.72 mm) here) or column. At cutoff, the ultimate axial load and moment are 1,330 kips (5915.84 kN) and 2,665 k.in. (301.09 kN-m), respectively. The maximum moment resistance is 4,155 k.in. (469.43 kN-m), which is mobilized at an axial load of about 750 kips (3336 kN). According to oral communication from FDOT, the maximum design capacity, as determined by soil conditions, never exceeded 600 kips (2668.8 kN).

The interaction diagram indicates the point where the steel changes from being elastic to inelastic. It should be noted, however, that the steel is inelastic below the yield point, and as the load increases, the steel stress decreases. When $k=1.0$, the stress is the prestress, and it is minimum when the axial load is maximum. Accordingly, the conditions developing at the strength limit states are entirely different from those codified for the design of prestressed concrete beams, and should, therefore, not be applied.

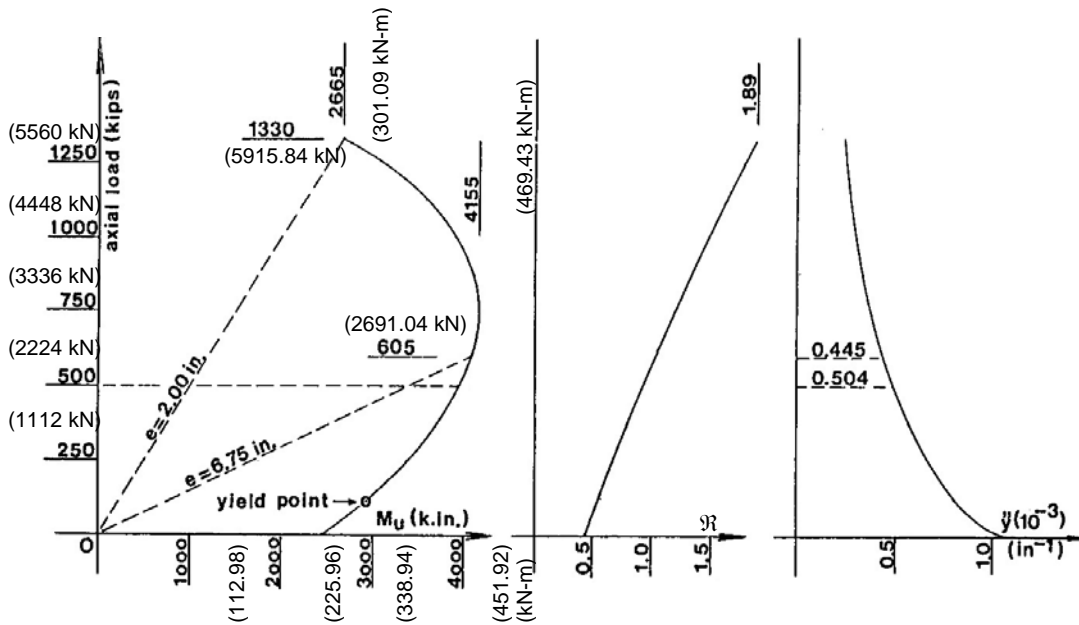


Figure 6 Interaction diagram for 18in. (45.72 cm) square pile

Also shown in

Figure 6 is the “k” diagram (such that ‘kd’ is the depth of the compressive stress diagram). From 0.479 at zero axial load, it increases in a nearly linear fashion to 1.89 at the cut-off point. It may be noted that the cross section would be fully in a state of compression at k=2.0. Indicated on the right hand side is the second derivative, (y''), of a deflection curve, which is also the rotation of the column per unit length, and the inverse of which is the radius, “ \mathcal{R} ”, of curvature. At $Q=500$ kips (2224 kN), $\mathcal{R}=1 \div 0.504 \times 10^{-3} = 1,984$ in. (50.39m). If the free length of the column is 16.0 ft. (4.88 m), the central deflection can be calculated as 2.32 inches (5.89 cm), and with 40.0 ft. (12.192 m), as 14.51 inches (36.86 cm). These figures indicate high-level flexibility, and the fact that P/Δ effects cannot be avoided at the strength limit states.

The performance of a cross section between zero and ultimate loads can be demonstrated by either taking the axial load or the eccentricity constant. Figure 7 demonstrates the development of moments for zero and 500-kip (2224 kN) axial loads as functions of “ α ” for both the CPCWMR and the traditional designs. It can be seen that for pure flexure ($Q=0$), the traditional design produces slightly higher moment than the CPCWMR at the beginning; but at ultimate, the CPCWMR takes over. For $Q=500$ kips (2224 kN), the CPCWMR is marginally lower than the traditional design for the whole valid strain spectrum.

A number of other observations could also be made in general for prestressed columns. Under axial load, the curve keeps on rising to the ultimate; a flat plateau would be undesirable for flexible columns relative to P/Δ effects.

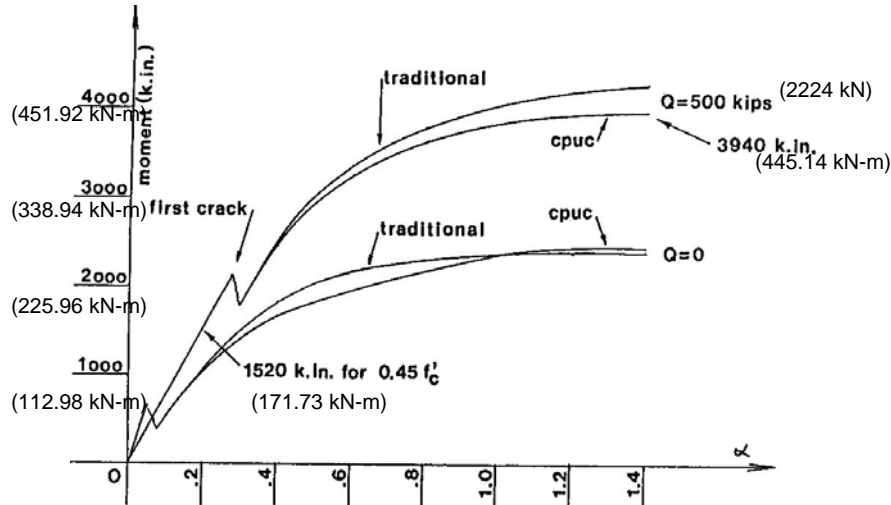


Figure 7 Moments for constant axial force

The moment for $0.45 f'_c$ at the service limit state is 1,520 k.in. (171.72 kN-m). The resistance at the strength limit state is 3940 k.in. (445.14 kN-m) or 2.59 times the previous figure, which suggests that such a service limit state is unnecessary. This limit state is also not being associated with any benchmark on the curve. It is meaningless and should, therefore, be eliminated from the design of prestressed columns and piles.

Similar to that of any prestressed concrete component, the curve suddenly drops upon first cracking, and then rebuilds itself as the strain increases. No matter what happens, the curve will never return to the initial cracking point, as the concrete has lost its tensile strength, and the resulting crack will open up at a lower load, which renders the first crack as a service limit state completely invalid and without a defensible objective. The CPCWMR column is not really susceptible to corrosion, yet uncontrolled crack openings may not be desirable. Since corrosion is a time-dependent action, the cracking limit state should be replaced by a crack-opening limit state for which only permanent force effects, but including those due to shrinkage, creep, and settlement, should be considered.

Figure 68 demonstrates the development of axial force as a function of " α " for an eccentricity of 6.75 in. (171.45 mm), which corresponds to 1.50 in. (3.81 cm) offset for the 4 in (10.16 cm) x 4 in. (10.16 cm) specimens used in the column tests of this project. The curve is similar in nature to those shown in Figure 7. Again, first cracking is immediately followed by inelastic action. Deformation of a 141.75 in. (3.6 m) long column, which corresponds to the tested specimens, yields a transverse deformation of 1.09 in. (27.69 mm),

increasing the maximum eccentricity to 7.84 in. (19.91 cm). This intercepts the interaction curve at a lower point. The maximum deformation “ y_0' ” can be calculated from Equation 1.

$$48\mathfrak{R} y_0^2 + [48\mathfrak{R}\iota - 5\iota^2] F_0 - 6\iota e = 0 \quad (1)$$

where: \mathfrak{R} = radius of curvature ($1 \div \gamma''$)
 e = initial eccentricity
 ι = length of hinged column

As “ e ” is not constant, the actual “ y_0 ” can only be obtained by successive approximation. In this case, the final values are as follows:

$$y_0 = 1.25 \text{ in. (31.75 mm), } Q = 490 \text{ kips (2179.52 kN),}$$

$$M = 3,920 \text{ k.in. (442.88 kN-m), } \mathfrak{R} = 1,960 \text{ in. (49.78 m)}$$

This calculation indicates that the investigation for P/Δ effects in the inelastic phase can be reduced to simple geometrical manipulations.

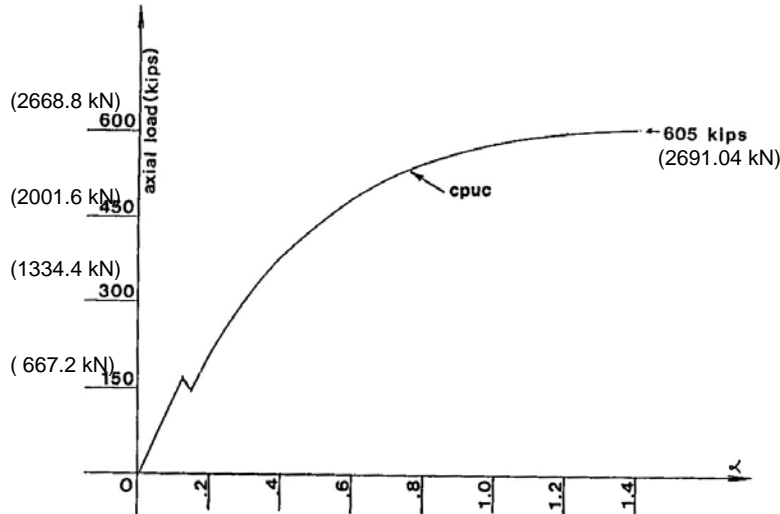


Figure 8 Axial load for an eccentricity of 6.75 in. (17.145 cm)

Column Tests (Series “B”, “C”, “D” and “E”)

In order to compare the performance of the CPCWMR design with that of reinforced columns and traditionally prestressed components, a total of 16 valid compression tests were carried out. All test specimens were 4” (10.16 cm) x 4” (10.16 cm) x 29” (73.66 cm) stubs of nominal 5,000 psi (34475 kN/m²) concrete. The specimens were prepared based on FDOT design mixes. Columns were tested under compression with eccentricities of 0.0, 0.75, 1.5, and ±1.50. The ± indicates load eccentricities in opposite directions. Effective length of tested columns is 32.0 in. (81.28 cm), providing an l/r ratio of 27.7. A typical column test set up is shown in Figure 9.

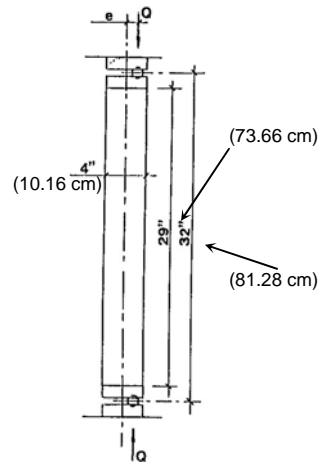


Figure 9 Schematic of test specimens

Hinge Tests

Hinges were tested to study the compressive strength and moment-rotation characteristics. This test series consists of three sets of tests with different filling material, such as concrete, silica sand, and carborundum. Each set consisted of four tests, with different diameter-to-height of hinge ratios such as 10.0, 5.0, 2.5, and 1.0. The hinge specimen consisted of steel inner and outer rings of 1.92 in. (4.88 cm) and 2.88 in. (7.32 cm) diameters. The annular space was filled with different fillers. The filler area was 3.62 in^2 (84.54 cm^2). At both ends of the hinge, there was a recess of 0.25 in. (6.35 mm) to accommodate the compression, which ensured load transfer only through the hinge filler (see Figure 10); the inner and outer rings were used only to provide confinement to the filler. Sufficient clearance was given between the compression rings and its contact surface with inner and outer rings to avoid the possible constraint during lateral loading or, to allow unrestrained rotation.

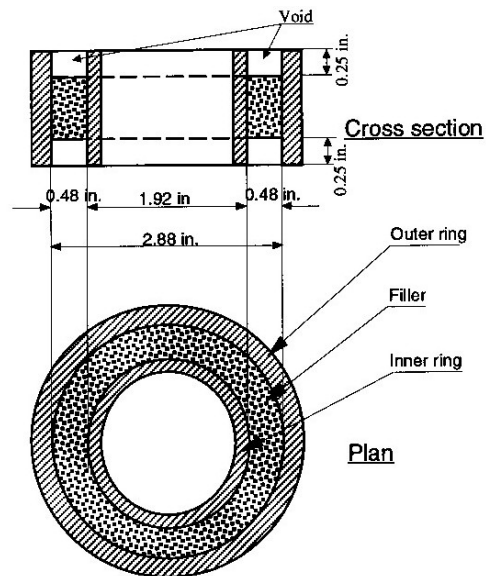


Figure 10 Hinge details

The first set of specimen fillers were made of 5000 psi (34475 kN/m²) concrete. The hinge heights were 1 (2.54), 1.5 (3.81), 2 (5.08), and 2.5 in. (6.35 cm) and the corresponding core heights (filler heights) 0.5 (1.27), 1 (2.54), 1.5 (3.81), and 2 in. (5.08 cm). The second and third sets of hinges were filled with silica sand and carborundum respectively. These sets of hinges had the same height as the first set. The experimental test set up for hinge test is given in Figure 11.

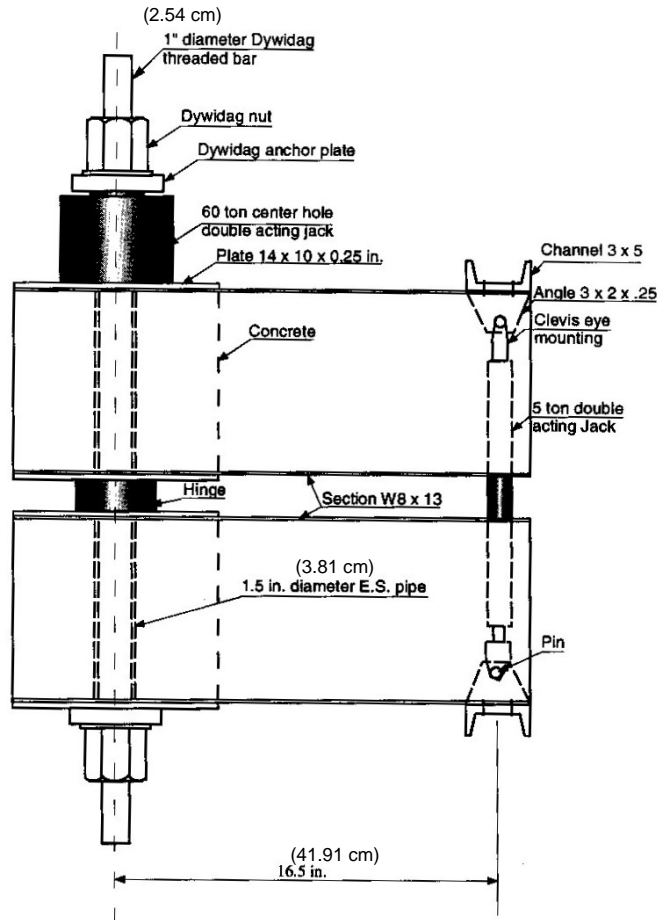


Figure 11 Experimental setup for hinge test

TEST RESULTS AND DISCUSSION

Column Tests:

Test specimen details and their failure loads are given in Table 1. Photographs of some of the failed columns are shown in Figure 12 and the load-deflection curves for columns are given in Figure 13.

Table 1 Column Test Specimens and Test Results

Test Series *	Type	Steel	Prestress (ksi)	Eccentricity (in.)	Trans. Steel	Failure Mode	Failure Load (kips)
C1	Plain	None	None	0.00	None	Crushing at Mid Point	97.9
C2	Plain	None	None	0.75	None	Inclined Failure Plane	64.1
C3	Plain	None	None	1.50	None	Inclined Failure Plane	21.0
C4	Plain	None	None	±1.50	None	Inclined Failure Plane	21.0

B1	Traditional	4-#3 Bars (2.76%)	None	0.00	Spiral	Partial Vertical Split	91.5
B2	Traditional	8-#3 Bars (5.52%)	None	0.00	Spiral	Unidentified	110.6
B3	Traditional	12-#3 Bars (8.28%)	None	0.00	Spiral	Unidentified	124.2
B4	Traditional	4-0.167" ϕ Wires	0.75	0.00	None	End Crushing	90.1
B5	Traditional	4-0.167" ϕ Wires	0.75	0.75	None	Compressive Crushing	56.6
B6	Traditional	4-0.167" ϕ Wires	0.75	1.50	None	Compressive Crushing	24.5
D1	CPCWMR	4-0.167" ϕ Wires	0.75	0.00	None	Cmp. Failure at center	110.6
D2	CPCWMR	4-0.167" ϕ Wires	0.75	0.75	None	End Crushing	65.9
D3	CPCWMR	4-0.167" ϕ Wires	0.75	1.50	None	End Crushing	27.4
D4	CPCWMR	4-0.167" ϕ Wires	0.75	± 1.50	None	Failure at End Plate	41.4
E1	CPCWMR	6-0.167" ϕ Wires	1.50	0.00	None	Crushing at Center	98.9**
E2	CPCWMR	6-0.167" ϕ Wires	1.50	0.75	None	Incl. Failure at Center	61.1**
E3	CPCWMR	6-0.167" ϕ Wires	1.50	1.50	None	Crushing at End Plate	29.7**
E4	CPCWMR	6-0.167" ϕ Wires	1.50	± 1.50	None	Failure at End Plate	22.7**

Note: * Each series is supplemented by three 4 x 12 inch control cylinders

** Columns are tested at 17 days and hence are extrapolated based on test results of control specimens tested at different date to get 28 days failure load



Figure 12 Some of the columns after testing curves

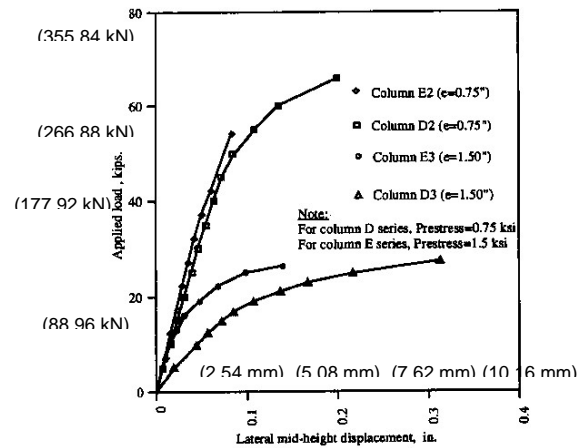


Figure 13 Load-deflection

The first comparison can be made among the specimens C1, B1, B2, and B3, all tested with (near) zero eccentricity. Failure loads are given in Table 1, and the results illustrated on the left hand side of Figure 14. They actually confirm the original FDOT tests values, shown on Figure 14 (b), in that the steel initially reduces axial resistance, and that it takes a considerable amount thereof to regain the loss. Potential resistance lines, tied to the tested plain concrete column C1, indicate as to what might happen if the steel and concrete were structurally compatible at failure. Test results fall at about three quarters, and the LRFD factored resistance at about one half, respectively, of the potential line. The low LRFD values are understood to cover unintended and uncontrollable small eccentricities. The designer cannot improve upon the performance of reinforced columns, as no accepted model exists, by which the interaction between the steel and concrete in the inelastic phase could adequately be described.

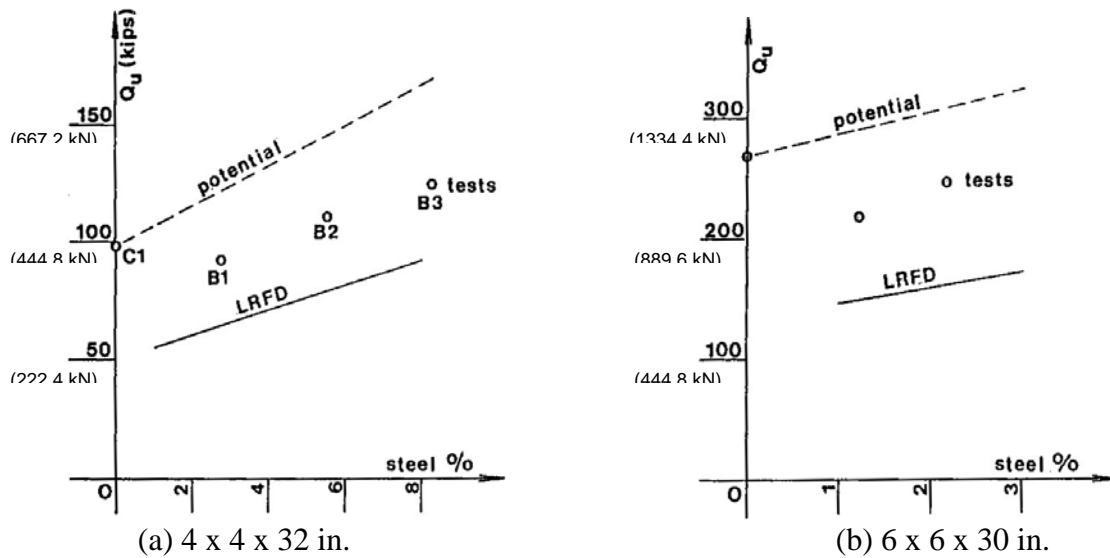
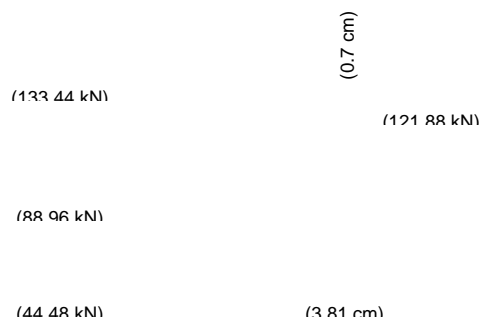


Figure 14 Performance of reinforced columns

Figure 15 illustrates the force-deflection diagram obtained from the CPCWMR specimen D3. It failed at a load of 27.4 kips (121.88 kN), acting with an eccentricity of 1.50 in. (3.81 cm). D3 can be considered as a 1:4.5 scale model of the 18 in. (45.72 cm) pile investigated under inelastic analysis of CPCWMR columns, yielding strength of 490 kips (2179.52 kN) at a deflection of 1.25 in (31.75 mm) (see Figure 8). After adjusting for the difference in f'_c (6,690 vs. 6,000 psi) (46127.55 vs. 41370 kN/m²) and applying scale factors, these translate, as shown in Figure 15, to 26.9 kips (119.65 kN) and 0.278 in. (7.06 mm). The specimen failed in two steps: The first crack occurred at a load of 19.2 kips (85.4 kN), and there was no further visible action until failure, at which time, a triangular piece, with side angles approximating 20° to the center line, broke out of the specimen. This mode of failure is similar to that for prestressed concrete beams. This, and the good correlation between predicted and tested values, indicate that, in terms of reliability and thus resistance factors, the CPCWMR column may be treated at ultimate limit state as a prestressed concrete beam.

For components in which the steel does not yield at failure, it is customary to define ductility as the ratio of the deformation at ultimate and the projected (virtual) elastic deformation. As shown in Figure 15, these values are 0.278 and 0.0618 in. (7.06 and 1.57 mm), respectively, producing an adequate ductility number of 4.5.



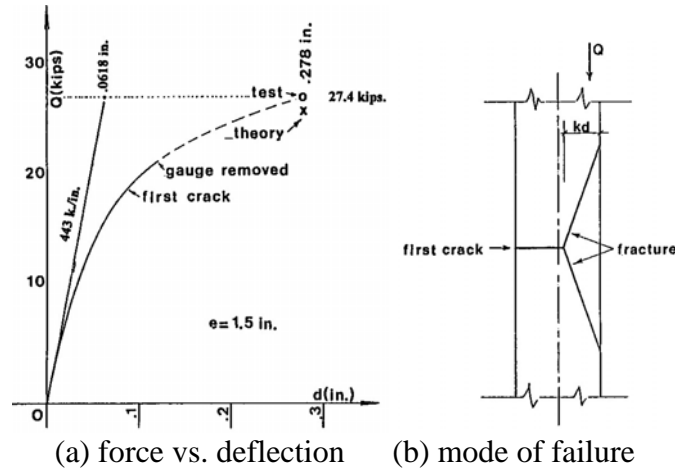


Figure 15 CPCWMR test D3

All control specimens were 4" (10.16 cm) x 12" (30.48 cm) cylinders. The 28-day strength of columns in Series "E" were obtained by extrapolation using test results of control specimens.

In Figure 16, comparisons are made between CPCWMR (D-Series) and traditionally prestressed columns (upper B⁻ series), and between CPCWMR columns with 0.75 ksi (5171.25 kN/m²) (D-Series) and 1.50 ksi (10342.5 kN/m²) (E-Series) prestress. The CPCWMR-D1 specimen with zero eccentricity carried a load of 110.6 kips (491.95 kN), or $f'_c = 6,812$ psi (46,968.74 kN/m²), which is above the average for 4" (10.16 cm) x 12" (30.48 cm) cylinder tests of 6,690 psi (46127.55 kN/m²). Even if D1 is discounted as an extreme, the CPCWMR curve is consistently higher than the traditional one, faring better than expected by analysis. The resistance of the CPCWMR specimens with 0.75 ksi (5171.25 kN/m²) prestress was marginally higher than those with 1.50 ksi (10342.5 kN/m²), except in the area of high eccentricity. This is quite natural as the part of the prestressing force that remains due to the axial load is from the compressive resistance of the concrete. With higher eccentricity, the flexural effects tend to dominate, and the higher flexural resistance reflects the influence of more steel being present. It is obvious that the level of prestressing in prototype construction should be kept to the minimum, which satisfies flexural requirements.

The CPCWMR member was also tested under mid-point lateral load (three point load) for flexure and four-point load for pure shear. These tests were carried out in universal testing machine at Florida Atlantic University. The maximum moment at first crack was 19.9 kip-in. (2.248 kN-m), which is 80% of the calculated based on the ultimate strength approach using rectangular stress distribution and about 165% of the flexural strength of that based on the cracking stress approach. The moment at failure is 41.9 kip-in. (4.734 kN-m). The crack was completely closed after the load is released and the crack pattern was similar to that of any RC or PC members. The shear failure was not adequately demonstrated, possibly because of inadequate distance between the load and support to develop shear failure.

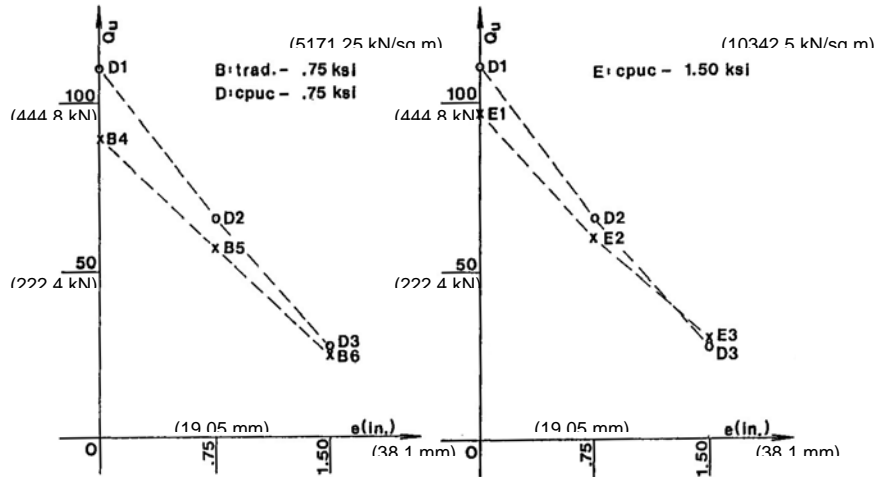


Figure 16 Comparisons of axial resistance

Hinge Tests:

The typical load-deformation behavior of hinges is shown in Figure 17. However, this behavior was not complete, because it was based on limited axial loading. Typical moment-rotational behavior of hinge under applied half cycle moment, and moment hysteresis of hinges are given in Figures 18, 19, and 20.

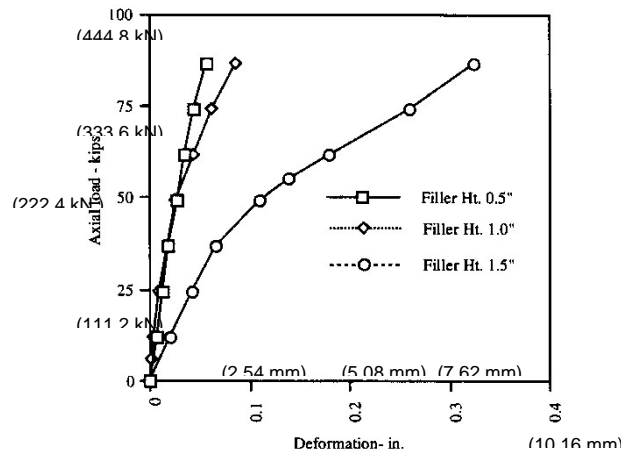


Figure 17 Load-deformation plot for hinge

The hinge seems to behave elastically until the filler fails or loses its stiffness and behaves elasto-plastically as the moment increases, and finally reaches the plastic stage as the filler stiffness shifts from the compression zone to the tension zone with no moment increase. On reversal of the loading, after the acting moment becomes smaller than the moment under plastic flow, the hinge returns to the elastic state. Under reversal of load, the hinge fill itself becomes an elasto-plastic medium with infinite reversibility and no sign of damage. It was expected that the higher width to depth ratio leads to a condition of perfect triaxial compression and resulting high compressive strength.

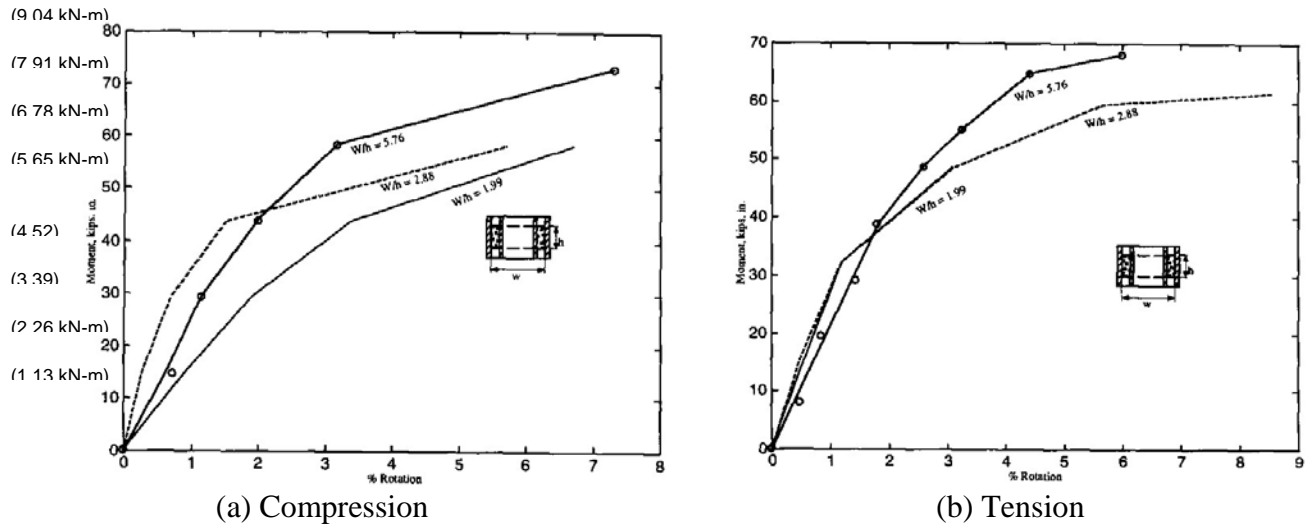


Figure 18 Variation of moment-rotation behavior for different w/h ratios of concrete hinge: I half-cycle

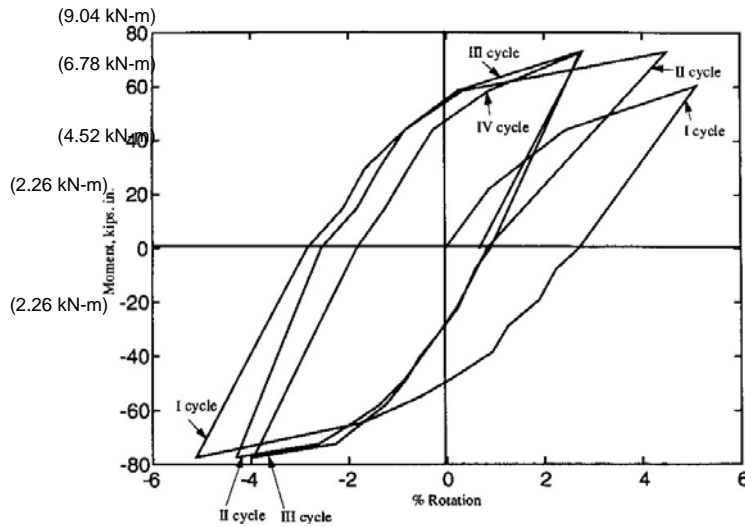


Figure 19 Moment-rotation hysteresis for concrete hinge with filler height of 0.5 in. (12.54 mm)

Hysteresis loops for a typical concrete hinge show that the rotation is about $\pm 4\%$. This is high enough to mitigate the dynamic force effects on columns during earthquakes. The reduction in rotation in the inelastic state over the load cycle is negligible and the moment capacity reaches almost a constant value. Generally, granular materials have better compressive strength when properly compacted and also the sliding movement of the granular particles after failure allows better energy dissipation by allowing more rotation.

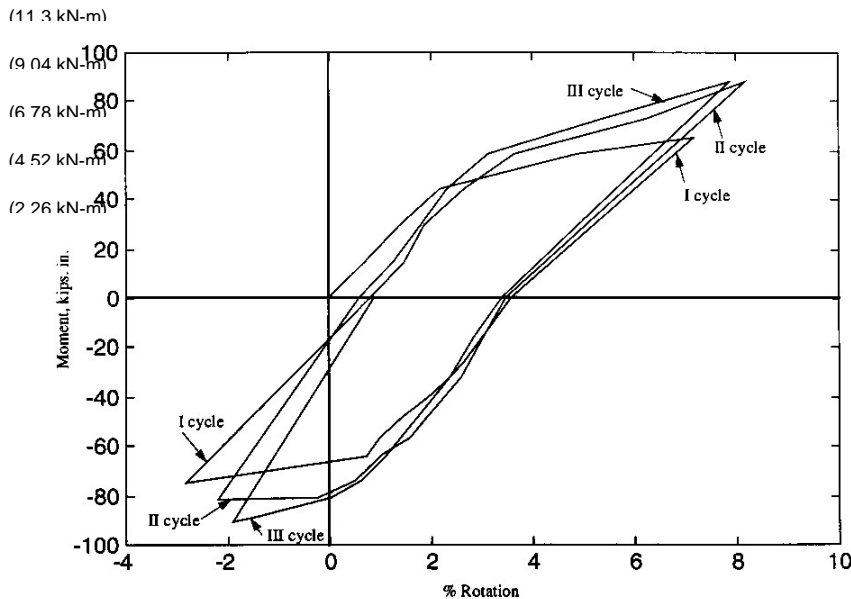


Figure 20 Moment-rotation hysteresis for silica sand hinge with filler height of 0.5 in.

CONCLUSIONS

Column and Hinge Tests:

Test results from thirty-seven concrete specimens in series 'A' of various sizes and strengths, which are not reported in this paper, seem to confirm one of the basic tenets of this innovative idea that the absence of reinforcement eliminates the loss of cover, i.e., premature failure of concrete column. The observed failure patterns in all the specimens of series 'A' approximate the failure angle predicted by Csagoly(1994). This angle was best demonstrated in the slender 4 x 12 in. (10.16 cm x 30.48 cm) cylinder, probably because for this the fracture mechanics was least disturbed by the interface confinement by the platens.

All the tested CPCWMR columns showed higher ultimate strength (about 10 to 20% as shown in Table 1) compared to conventional prestressed columns. This was due to the loss in the internal moment arm being more than compensated by having all the steel in tension at center. At large eccentric load, the increase of prestress increases the ultimate strength of the CPCWMR column. However, prestress is detrimental to the compressive strength of the column at no or small load eccentricity as shown in Figure 16. Hence, the level of prestressing in the prototype construction should be kept to the minimum, which satisfies the flexural requirements.

The failure patterns of CPCWMR columns were similar to those for conventional prestressed columns reported by Carinci and Halvorsen (1987). The columns failed by sudden crushing on

the compression side at about 0.14 times the length from one of the ends. This was followed by diagonal cracking extending to the tension face through the column core. CPCWMR members under pure flexure (beam bending) and shear loading failed at higher ultimate strengths than those determined analytically. Though these test results clearly evidence the ductility behavior of the CPCWMR columns, under large deformations like those induced during earthquakes, special devices may be required to dissipate the additional energy stored.

The modified Freyssinet type hinge, called the Extended Flexural Device (EFD) for CPCWMR column, demonstrated excellent in energy dissipating characteristics. Tests on a total of six hinges, with three different filler materials and three different heights, confirmed that the above parameters definitely affected the moment-rotation performance of the hinges. The moment-rotation behavior of these hinges was similar to that for under-reinforced concrete beams in flexure. The filler sustained a strain level of 25,000 psi (172375 kN/m²). Linear behavior was observed up to the strain level of about 4% followed by inelastic behavior up to 8%. The moment-rotation behavior converges to a constant after a few load cycles and survives a number of complete moment reversals without any sign of damage. The moment carrying capacity and compressive strength increase as the width-to-height ratio increases. The harder-granular-filler material showed better performance in terms of moment-rotational and compressive strength capability.

As a whole, the combination of CPCWMR column and this new hinge seems to be the best alternative for the column in the marine and seismic environment. In addition to the observed increase in compressive strength and ductility, the CPCWMR columns will provide more corrosion resistance due to large cover and possible better compaction of the concrete (so that high density concrete is possible). The hinges provide extended flexural capacity and over-load protection to the column in seismic conditions. It is possible that the plastic plateau of the curve for hinge can be set at any desired level, i.e. about 75% of the flexural strength of the column, by which the column will not only be protected against both shear and flexural failure due to seismic action, but would also resist the moments generated by gravitational loads without excessive deformation. The observed moment-rotation curve can be modeled bilinearly, i.e., with the rising part pseudo-elastic and the plateau fully inelastic. It considerably reduces the column stiffness and permits easy inelastic design and elimination of the arbitrary strength reduction factor for the column.

ACKNOWLEDGMENT

This paper is based on a National Cooperative Highway Research Program funded project #20-37 "Centrally Prestressed, Unreinforced Concrete Columns and Piles" (Contract Monitor: Dr. K. Thirumalai, P.I.: Dr. D. V. Reddy, and Consultant: P. F. Csagoly). Grateful acknowledgments are due to Paul F. Csagoly, President, Structural Research and Development Engineering, Clearwater, FL, for formulation of the innovative project, participation, and careful monitoring of the investigation. Gratitude is expressed to Dr. K. Thirumalai for his support and encouragement. Thanks to Ms. Diana Arboleda for her patient and excellent editorial work.

Bibliography

- Carinci, C. A. and Halvorsen, G. T., "Tie Requirements for Prestressed Concrete Columns," PCI Journal, Vol. 32, No. 4, July-August 1987, pp.46-79.
- Csagoly, P. F., "End effect on the Orientation of the Failure Plane for Compressively Loaded Cylinder and Prismatic Specimens," Unpublished, 1994
- Cusson, D. and Paultre, P., "High Strength Columns Confined by Rectangular Ties," Journal of Structural Engineering, ASCE, Vol. 120, No. 3, March 1994.
- Elias, H. E. and Durrani, A. J., "Confinement of Prestressed Concrete Columns," PCI Journal, Vol.33, No. 3, May-June 1988, pp.123-141.
- Ichinose, T., "Splitting Bond Failure of R/C Columns under Seismic Action," ACI Structural Journal, Vol. 92, No. 5, 1996, pp. 535-542.
- Mander, J. B., Priestley, M. J. N., and Park, R., "Theoretical Stress-Strain Model for Confined Concrete," Journal of Structural Engineering, ASCE, Vol. 114, No. 8, August 1988.
- Ranade, S. and Reddy, D. V., "Computer Modeling for Chloride Diffusion of Reinforced Concrete Beams in the Marine Environment," Proc. International Conf. On Corrosion and Corrosion Protection of Steel in Concrete, Sheffield, England, July 24-28, 1994, pp. 648-657.
- Razvi, S. R. and Saatcioglu, M., "Strength and Deformability of Confined High-Strength Concrete Columns," ACI Structural Journal, Vol.91, No. 6, November-December 1994, pp. 678-687.
- Sheikh, S. A. and Uzumeri, S. M., "Strength and Ductility of Tied Concrete Columns". Journal of Structural Division, ASCE, Vol. 106, No. ST5, May 1980, pp. 1079-1102.
- Uomoto, T. and Misra, S., "Behavior of Concrete Beams and Columns in Marine Environment when Corrosion of Reinforcing Bars takes Place". Proceedings of Second International Conference St. Andrews by-the-Sea, Canada 1988, ACI, SP-109, pp. 127-146.
- Zia, P., and Moreadith, F. L., "Ultimate Load Capacity of Prestressed Concrete Columns," ACI Journal, Vol.63, No. 7, July 1966, pp. 767-788.

Notation

- A = internal moment arm
 e = initial eccentricity
 f'_c = concrete compressive strength
 g = distance between center of compression block and center of top steel
 H_s = tendon force
 kd = depth of compressive stress diagram
 l = length of hinged column
 M = moment
 M_c = first moment relative to the neutral axis
 M_u = ultimate flexural capacity
 N_c = vertical compressive force
 q = between center of compression block and center of steel
 Q = axial Load
 Q_u = ultimate axial capacity
 R = radius of curvature
 R_D = dead load reaction
 y_0 = maximum deformation
 y'' = second derivative of deformation
 α = ratio between the actual concrete strain and strain associated with f'_c

List of Tables

Table 1 Column Test Specimens and Test Results

List of Figures

- Figure 1 Observed spalling of concrete covers
 Figure 2 Traditional and proposed cross sections
 Figure 3 Comparison of flexural resistance
 Figure 4 Modified Freyssinet type hinge
 Figure 5 Distribution of compressive stresses as function of α
 Figure 6 Interaction diagram for 18in. square pile
 Figure 7 Moments for constant axial force
 Figure 8 Axial load for an eccentricity of 6.75 in.
 Figure 9 Schematic of test specimens
 Figure 10 Hinge details
 Figure 11 Experimental setup for hinge test
 Figure 12 Some of the columns after testing
 Figure 13 Load-deflection curves
 Figure 14 Performance of reinforced columns
 Figure 15 CPCWMR test D3
 Figure 16 Comparisons of axial resistance
 Figure 17 Load-deformation plot for hinge
 Figure 18 Variation of moment-rotation behavior for different w/h ratios of concrete hinge
 Figure 19 Moment-rotation hysteresis for concrete hinge with filler height of 0.5 in.
 Figure 20 Moment-rotation hysteresis for silica sand hinge with filler height of 0.5 in.